OncoTargets and Therapy

Dovepress
open access to scientific and medical research

Open Access Full Text Article

ORIGINAL RESEARCH

Huaier Restrains Cholangiocarcinoma Progression in vitro and in vivo Through Modulating lncRNA TP73-AS1 and Inducing Oxidative Stress

This article was published in the following Dove Press journal:
OncoTargets and Therapy

Daolin Ji[1,2]
Wangyang Zheng[1,2]
Peng Huang[1,2]
Yue Yao[3]
Xiangyu Zhong[1]
Pengcheng Kang[1]
Zhidong Wang[1]
Guojing Shi[4]
Yi Xu[1,2]
Yunfu Cui[1]

[1]Department of Hepatopancreatobiliary Surgery, The Second Affiliated Hospital, Harbin Medical University, Harbin, Heilongjiang Province, People's Republic of China; [2]The Key Laboratory of Myocardial Ischemia, Harbin Medical University, Ministry of Education, Harbin, Heilongjiang Province, People's Republic of China; [3]Department of Endocrinology and Metabolism, The Second Affiliated Hospital, Harbin Medical University, Harbin, Heilongjiang Province, People's Republic of China; [4]Department of Biochemistry and Molecular Biology, Harbin Medical University, Harbin, Heilongjiang Province, People's Republic of China

Purpose: Huaier, the fruiting body of Trametes robiniophila Murr, is a kind of traditional Chinese medicine. Recently, many studies have confirmed that Huaier has antitumor effects on various malignancies. Moreover, studies have demonstrated that long noncoding RNAs play an important regulatory role in the occurrence and progression of malignancies. Our present study was to explore whether Huaier has a potential antitumor effect in cholangiocarcinoma and reveal the relationship between lncRNAs and Huaier-induced tumor inhibition.

Methods: Microarray assay was performed to identify the candidate lncRNAs regulated by Huaier. Quantitative real-time PCR was applied to assess the effect of Huaier on TP73-AS1 expression. The effect of Huaier on the cell viability, proliferation, migration and invasion was evaluated by CCK-8, colony formation, wound healing and Transwell assays, respectively. The ratio of cell apoptosis was determined using AO/EB, Hoechst 33342 and flow cytometry. The effect of Huaier on oxidative stress was revealed using DCFH-DA, mitoSOX, JC-1 probes and Western blotting. In addition, the effect of Huaier on tumor growth and metastasis was explored using subcutaneous tumor model and lung metastatic tumor model in nude mice.

Results: In vitro, Huaier inhibited the proliferation, migration and invasion of cholangiocarcinoma cells by down-regulating TP73-AS1 and induced apoptosis through mitochondrial apoptotic pathway. In vivo, Huaier suppressed the growth and metastasis of cholangiocarcinoma by modulating the expression of proliferation and EMT-associated proteins.

Conclusion: Huaier could inhibit cell proliferation, invasion and metastasis by modulating the expression of TP73-AS1, meanwhile promote apoptosis of CCA cells through disturbing mitochondrial function, inducing oxidative stress and activating caspases in vitro. In addition, Huaier could suppress tumor growth and metastasis by regulating the expression of proliferation and EMT-related proteins. In the meantime, Huaier prolonged the survival of nude mice in lung metastatic model with acceptable drug safety.

Keywords: cholangiocarcinoma, Huaier, TP73-AS1, oxidative stress, apoptosis

Introduction

Cholangiocarcinoma (CCA), a highly aggressive cancer originating from the epithelial cells of bile ducts, ranks the second most common malignancy in hepatic primary diseases worldwide.[1,2] Epidemiological surveys indicated that the morbidity and mortality rates of CCA had noticeable ascendant trend around the world, particularly in Asia and America.[3] At present, surgical resection and chemotherapy still remain the main therapeutic strategies for patients with CCA, but both have

Correspondence: Yunfu Cui; Yi Xu
Department of Hepatopancreatobiliary Surgery, The Second Affiliated Hospital, Harbin Medical University, 246, Xuefu Road, Harbin, Heilongjiang Province 150086, People's Republic of China
Tel +86 451-86605113
Email yfcui777@hotmail.com; xuyihmu@163.com

submit your manuscript | www.dovepress.com
DovePress
http://doi.org/10.2147/OTT.S257738

their own limitations. Due to the insidious onset, the lack of early specific clinical manifestations and rapid progression, most patients with CCA are usually diagnosed at the late stage and lost the opportunity of early surgical treatment.[4] However, for those patients who have had access to radical resection at early stage, the high recurrence rate still should not be ignored.[5] Chemotherapy is the hope for patients with advanced or recurrent CCA, such as cisplatin combined with gemcitabine is the current first-line chemotherapy strategy for patients with advanced CCA.[6,7] Whereas, primary resistance, secondary resistance and adverse drug reactions often occur during therapy, which leads to interruption of chemotherapy and leaves the patients with poor prognosis.[6,7] Statistical data indicated that these limitations resulted in a 5-year survival rate of less than 15% for CCA patients.[8] Therefore, the investigation for novel effective and lower toxic anti-tumor drugs has become the active demand to improve the clinical outcomes of CCA.

In recent years, natural phytochemicals have attracted the attention of researchers as potential anti-tumor agents. Among them, more and more traditional Chinese medicine (TCM) which have anti-tumor properties have been discovered and investigated.[9–12] Huaier, the fruiting body of Trametes robiniophila Murr, is a kind of light-tawny mushroom parasitic on the boles of locust trees.[13] According to the records of TCM, Huaier is usually used as an anti-inflammatory.[14] As pointed out in recent explorations, Huaier extract could play an anti-tumor role in a variety of malignant tumors, such as gastric cancer, lung cancer, osteosarcoma and breast cancer.[15–18] Meanwhile, Huaier could also strengthen the organic immunity by up-regulating the activity of natural killer cells and T cell subsets.[19] Although the role of Huaier in some common malignancies has been reported in scatter studies, the potential effect and exact mechanism in human CCA are still not fully revealed.

Long non-coding RNAs (lncRNAs) are defined as a family of RNA molecules with transcript length over 200 nt.[20] Instead of encoding for proteins, they play important roles as a considerable layer of cell biological regulation, such as epigenetic regulation, transcriptional regulation and post-transcriptional regulation.[20] Many studies have indicated that lncRNAs could play crucial roles in regulating the growth of normal tissue, cell differentiation, and tumor progression.[21–23] In addition, aberrant expression levels of lncRNAs have been coupled with various malignancies including CCA.[21–23] Moreover, with the development of high-throughput sequencing technology, a tremendous amount of tumor-related lncRNAs have been recognized and studied.[24,25] In addition, studies on anti-tumor agents have been gradually linked with the impact on lncRNAs expression.[26]

In our present research, different human CCA cell lines as well as different experimental animal models were applied to explore the functional role of Huaier extract in vitro and in vivo and discover its underlying mechanisms. Additionally, high-throughput sequencing assay was performed to analyze the effect of Huaier on lncRNAs expression. Our experimental data illustrated that Huaier could not only inhibit cell proliferation, migration and invasion but also induce apoptosis by up-regulating intracellular ROS levels in vitro. Moreover, Huaier could significantly suppress tumor growth and metastasis in vivo. These effects of Huaier might be associated with down-regulation of lncRNA TP73-AS1, mitochondrial dysfunction and caspase cascade activation.

Materials and Methods

Reagents and Antibodies

Roswell Park Memorial Institute (RPMI)-1640 medium was bought from HyClone (Logan, UT, USA). Fetal bovine serum (FBS) was obtained from Thermo Scientific (Gibco, Shanghai, China). Cell counting kit-8 (CCK-8) was obtained from Dojindo Molecular Technologies (Tokyo, Japan). Dimethyl sulfoxide (DMSO) and Hoechst 33342 staining solution were purchased from Solarbio (Beijing, China). Primary antibodies against Bcl-2, Bax and cytochrome c were supplied by Proteintech (Rosemont, IL, USA). Anti-cleaved caspase-9 and anti-cleaved caspase-3 antibodies were purchased from Cell Signaling Technology (CST, Danvers, MA, USA). Antibodies against Ki-67, PCNA, Snail, E-cadherin, Vimentin and N-cadherin were acquired from Abcam (Cambridge, MA, USA).

Drugs

Aqueous Huaier extract used in the present experiments was supplied by Gaitianli Pharm (Qidong, China). Huaier extract was dissolved in RPMI-1640 medium at the concentration of 100 mg/mL. Then, the diluted solution was sterilized with filter (aperture of 0.22 μm) and stored as the stock solution in the −80°C refrigerator away from light. The stock solution was diluted to target concentration with a complete medium during the experiment. To avoid repeated freezing-thawing cycles that might affect the

effectiveness of the drug, the stock solution needed to be repackaged and replaced every two freezing-thawing cycles.

Cell Culture

The human CCA cell line RBE was commercially bought from Shanghai Institute of Biological sciences and Cell Resources Center, Chinese Academy of Sciences (Shanghai, China). CCLP1 and HuCCT1 were kindly donated by Prof. LX Liu (the First Affiliated Hospital of Harbin Medical University). These three cell lines were cultured in RPMI-1640 medium added with filtered FBS (10% concentration), penicillin (100 U/mL) and streptomycin (100 mg/mL). All the cells were maintained in humid cell incubator at 37°C containing 5% CO_2. In addition, monthly mycoplasma testing was performed to ensure mycoplasma-negative culture. In the present research, the use of the cell lines was approved by the Ethics Review Committee of Harbin Medical University.

Cell Viability Assay

The effect of Huaier on the viability of human CCA cell lines CCLP1, HuCCT1 and RBE was evaluated using CCK-8 assays. Tumor cells at the exponential growth stage were seeded into 96-well culture plate at the inoculum density of 5×10^3 per well. After 24 hours of continuous culture in the incubator, the previous medium was discarded and replaced with medium containing Huaier at different concentration gradients, and then the cells were incubated for another 24 h or 48 h. Next, 10 μL of CCK-8 working solution was added to each well. After incubation for 2 h, the absorbance at 450 nm was detected with a multifunction microplate reader (CLARIOstar; BMG LABTECH, Ortenberg, Germany). The specific calculation method was: Cell viability = (A_{450} of drug-treated well-A_{450} of blank well)/(A_{450} of non-drug-treated control well- A_{450} of blank well)×100.

Colony Formation Experiment

Colony formation assays were performed to assess the effect of Huaier on cell proliferation. Briefly, tumor cells pretreated with Huaier were inoculated into 6-well plate at the density of 1×10^3 cells per well. After 2 weeks of incubation, the cells were fixed with paraformaldehyde and stained with crystal violet staining solution. Next, the visible cell colonies (>50 cells/colony) were observed and assessed under a microscope (Olympus, Tokyo, Japan).

Cell Morphological Observation

After treated with different concentration gradients of Huaier in the presence or absence of NAC (3 mM), the morphological changes of CCLP1 and RBE cells were observed and photographed under a microscope.

Apoptosis Assay

Effect of Huaier on the apoptosis of CCA cells was preliminarily investigated by acridine orange/ethidium bromide (AO/EB) double fluorescent dye (Solarbio, Beijing, China) and Hoechst 33342 assay kit according to the reagent specifications. In the AO/EB experiment, tumor cells were pre-seeded and cultured overnight in a 6-well petri dish. After 24 h of stimulation with Huaier, the preconfigured AO/EB stain was added to each well. Finally, the apoptosis level was observed and evaluated under a fluorescent microscope system (Leica, Buffalo Grove, IL, USA). In Hoechst 33342 assay, the Huaier-treated cells were immobilized with paraformaldehyde solution and stained with Hoechst 33342 working solution for 20 min. Then, the intensity of blue fluorescence was observed and photographed by a fluorescence microscope.

To further confirm the effect of Huaier on cell apoptosis, Annexin V-FITC and PI double-staining apoptosis detection kit (BD Biosciences, Shanghai, China) was applied. In brief, 1×10^5 cells were seeded into 6-well plate and cultured overnight. Next, the cells were stimulated with different concentrations of Huaier with or without NAC. After 24 h of stimulation, the cells were collected using EDTA-free trypsin (Beyotime, Shanghai, China) and rinsed with 4°C precooled phosphate-buffered saline (PBS) before resuspended in the precooled 1×binding buffer. The total volume of each test sample was fixed to 500 μL. After that, cells were stained with Annexin V-FITC (5μL) and PI (5 μL). Finally, the cells were filtered with 300 aperture mesh and the cell apoptosis levels were evaluated by applying a flow cytometer (BD Biosciences, Franklin Lakes, NJ, USA).

Migration and Invasion Assays

The effect of Huaier on the migration rate of CCA cells was initially evaluated by wound healing assays. Briefly, a sterile 200 μL pipette tip was applied to make a scratch area on the cell layer of 6-well culture dish. Then, the floating cells around the scratch area are washed away with sterilized PBS, and the remaining cells were cultured in serum-free medium with or without Huaier. The motility

of each group was recorded at 24 h and 48 h. Transwell assays were performed to further determine the effect of Huaier on cell motility. Briefly, the Huaier-treated cells were inoculated in the upper chambers of the Transwell unit (Corning, NY, USA) and cultured with 200 μL of general culture medium without FBS. Then, 600 μL of culture medium containing 10% FBS was added to the lower chambers as a kind of coinducer. The chambers covered with or without Matrigel (BD Biosciences, San Jose, CA, USA) were used to monitor the cell invasion or migration, respectively. After 24 h incubation at 37°C, the cells still in the upper chambers were removed. Finally, the cells on the lower face of the Transwell chambers were fixed with 4% paraformaldehyde solution and stained with crystal violet staining solution. After air drying, the total number of stained cells was counted under a microscope.

Quantitative Real-Time PCR and Cell Transfection

The total RNA from CCLP1 cells treated with or without Huaier was extracted by applying TRIzol reagent (Merck, Shanghai, China) and the complementary strand of DNA (cDNA) was synthesized using 1μg total RNA with SuperScript III First-Strand Synthesis SuperMix Kit (Invitrogen, Shanghai, China). Polymerase chain reaction (PCR) assay was applied to explore the expression of specific lncRNA using fluorescence ration PCR instrument (Bio-Rad, Hercules, California, USA) with QuantiFast SYBR Green PCR Kit (Qiagen, Shanghai, China). The primer sequences of TP73-AS1 used in the PCR experiment were listed as follows: the forward sequence was 5'-CCGGTTTTCCAGTTCTTGCAC-3'; the reverse sequence was 5'-GCCTCACAGGGAAACTTCATGC-3' (Genechem, Shanghai, China). In this study, TP73-AS1 overexpression or TP73-AS1 knockdown was obtained via transfecting CCLP1 cells with TP73-AS1 vector or TP73-AS1 siRNA. The vector, siRNA and their corresponding controls were designed by GenePharma (Shanghai, China). Lipofectamine 3000 transfection reagent (Invitrogen, CA, USA) was applied for cell transfection following the protocol recommended by the reagent supplier. After 48 h of transfection, the cells were harvested for further research.

LncRNA Microarray Assay

The difference in lncRNA expressions between control groups and Huaier treatment (2.25 mg/mL) groups (CCLP1) was determined using the Human LncRNA Array V4.0 (Illumina, CA, USA). By utilizing the fourth-generation lncRNA sequencing technology, nearly 40,916 lncRNAs could be investigated. In addition, the microarray hybridization process was implemented following the manufacturer's standard technical procedures (Illumina, CA, USA). The process involved RNA sample extraction, RNA sample purification, cRNA transcription, cDNA labeling (Cy3-dCTP and Cy5-dCTP) and cDNA hybridized onto the LncRNA Array V4.0 (chip specification: 4×180K, ≥2 probes for each lncRNA). All the targeted sequences of lncRNA included in the microarray were compared and merged from authoritative databases, such as ENSEMBL, lincRNA catalog, LNCipedia, UCSC, lncRNAs from IBP, Non-coding RNA Search and so on. Hierarchical clustering was applied to analyze microarray sequencing data and differential screening of lncRNAs expression should conform to the following principles: the threshold values of differential expressions >2 or <2 fold change, meanwhile, $P < 0.05$.

Detection of Huaier-Induced Oxidative Stress

The oxidative stress induced by Huaier was evaluated via 2′, 7′-dichlorofluorescein-diacetate (DCFH-DA, Yeasen, Shanghai, China) and mito-SOX (Thermo Fisher Scientific, Waltham, MA, USA) fluorescence probes. Briefly, cells were grown in 96-well plate (2×10^4 per well) overnight. Then, the cells were exposed to the appropriate concentration of Huaier in the presence or absence of NAC or mito-TEMPO regents. Next, the cells were rinsed twice with PBS and coincubated with DCFH-DA or mito-SOX probes in RPMI-1640 medium for appropriate time (20 min for DCFH-DA, 30 min for mito-SOX). Finally, the cells were washed three times with prewarmed serum-free medium and the fluorescence intensity (bright-green for DCF and bright-red for mito-SOX) was detected under fluorescence microplate reader.

Detection of Mitochondrial Membrane Potential

Huaier-induced changes in mitochondrial membrane potential (MMP) were analyzed via the JC-1 fluorescent probe (Yeasen, Shanghai, China). When the MMP is normal (high level), JC-1 accumulates in the mitochondrial matrix, forming polymers and exhibiting bright-red fluorescence (excitation wavelength/550 nm, emission

wavelength/600 nm). Conversely, when the MMP declines, JC-1 cannot accumulate in the mitochondrial matrix, forming monomers and exhibiting bright-green fluorescence (excitation wavelength/485 nm, emission wavelength/535 nm). Therefore, the MMP could be evaluated by the changes in fluorescent signals. The degree of mitochondrial depolarization was routinely assessed by the relative ratio of red to green fluorescence signal intensity. Briefly, cells pretreated with Huaier were collected and resuspended in JC-1 working solution (diluted with serum-free medium). Then, the cells were cultured at 37°C for 20 min and rinsed with 1×binding buffer. Finally, the cells were suspended in 4°C precooled binding buffer and the intensity of the red and green fluorescence signals were detected by applying fluorescence microplate reader.

Evaluation of Intracellular Glutathione Level and Intracellular Thioredoxin Reductase Activity

Glutathione (GSH) is an important free radical scavenger in cell. When cells undergo oxidative stress, GSH (reduced state) is oxidized to GSSG (oxidative state). In this study, intracellular GSH and GSSG levels were detected using a reduced Glutathione assay kit (Solarbio, Beijing, China). Briefly, cells pretreated with Huaier were harvested and lysed with RIPA lysis buffer (Solarbio, Beijing, China). Then, the cells were further lysed using an ultrasonic oscillator for 1 min on the ice (ultrasonic power: 40%, frequency: processing 2 s and pausing 1 s). After that, the lysed liquid was centrifuged at 12,000 g for 15 min at 4°C and the supernatant was re-collected to a precooled 1.5 mL Eppendorf tube. The protein concentration was obtained by applying the Pierce Rapid Gold BCA Protein Assay kit (Thermo Scientific, Shanghai, China). Then, the intracellular total GSH and GSSG levels were analyzed using a microplate reader (wavelength/412 nm). The ratio of GSH to GSSG was used to evaluate the balance of the REDOX system.

Thioredoxin reductase (TrxR) is a crucial enzyme involved in the Trx antioxidant mechanism. In this research, the TrxR activity was analyzed via a TrxR activity detection kit (Solarbio, Beijing, China). Briefly, cells were pretreated with Huaier and the total proteins were extracted, the specific operation steps are the same as above. Finally, the TrxR activity was assessed using a 96-well plate under fluorescence microplate reader according to the reagent supplies manual.

Western Blotting

After 24 h of Huaier stimulation, cells were rinsed with precooling PBS and lysed with RIPA lysis buffer premixed phenylmethylsulfonyl fluoride (PMSF) and protein phosphatase inhibitor. After that, the mixture was collected with 1.5 mL Eppendorf tubes and centrifuged for 15 min (12,000 g, 4°C). Then, the supernatant was collected using another 1.5 mL precooled Eppendorf tube and the total protein concentration was measured. Proteins (total mass: 30 μg) were divided with SDS-PAGE (separating gel concentration ranging from 10% to 12%, stacking gel is 5%) and transferred to PVDF membrane (Thermo Scientific, Shanghai, China) with an aperture of 0.22 μm or 0.45 μm. After blocking with defatted milk (2.5 g milk powder dissolved in 50 mL TBST, final concentration 5%) at 37°C constant temperature shaker and incubation with primary antibodies against Bcl-2, Bax, cytochrome c, cleaved caspase-9, cleaved caspase-3 and GAPDH overnight at 4°C, the PVDF membranes were washed with TBST and coincubated with second antibodies at 20–22°C for another 1.5 h. Finally, the PVDF membranes containing target proteins were photographed using Super ECL Chemiluminescent Substrate Reagent Kit (Thermo Scientific, Shanghai, China) under a full-automatic chemiluminescence imaging analysis system (Tanon, Shanghai, China).

In vivo Experiment

The specific pathogen-free (SPF) BALB/c nude mice (female, aged 5–6 weeks, body weight 18–20 g) were bought from Beijing Charles River Laboratory Animal Technology Co. Ltd. In addition, the in vivo experiments were approved by the Animal Health Care and Use Committee of Harbin Medical University (Ethics approval number: SYDW2020-009) and the experimental procedures complied with the guideline of the Animal Health Care and Use Committee of Harbin Medical University. Before experimental operations, all the mice were acclimated to the new feeding environment for 4–5 days. To confirm the inhibitory effect of Huaier on CCA growth, CCLP1 cells (5×10^6 suspended in 100 μL sterilized PBS) were injected subcutaneously into the posterior axillary region of nude mice to establish subcutaneous tumor model. Next, the tumor volume was monitored and recorded every 3 days. The specific calculation equation of tumor volume is: $V = 0.52 \times L \times W^2$ (V, volume; L, longest diameter; W, width diameter perpendicular to longest diameter). The

experimental mice were divided into control group and therapeutic group (5 for each cohort) when the tumor volume reached approximately 80–100 mm^3. The control group was administrated with 200 μL of sterile saline by intragastric administration once a day, the therapeutic group was administrated with Huaier (3 g/kg dissolved in 200 μL sterile saline, intragastric administration, once daily). Changes in tumor volume were recorded continuously until close monitoring and intervention were performed for 31 days. Then, the mice were sacrificed. The subcutaneous tumor specimens were resected and divided equally into two parts: one part was immersed in paraformaldehyde, and the other part was kept at −80°C for further assays. A lung metastatic model was applied to determine the effect of Huaier on CCA metastasis. Ten mice were randomly assigned to two groups (5 for each cohort); then, 5×10^6 luciferase-labeled CCLP1 cells (suspended in 200 μL sterilized PBS) were injected into the nude mice through the caudal vein. Next, each group was given the same therapeutic interventions as above. After 46 days of therapy, the fluorescence intensity of nude mice in each group was detected using an in vivo bioluminescence imaging system (Bruker Optics, Germany). Next, the mice were euthanized and the lungs were dissected to compare metastasis between the two cohorts. In addition, the heart, liver, and kidney resected from the lung metastatic model were also preserved and immersed in paraformaldehyde for the next histological examination. Similarly, the effect of Huaier on body weight and survival time in nude mice was preliminarily assessed through lung metastatic model (6 nude mice per group). Body weight and survival were recorded and plotted until the end of the research.

Histology and Immunohistochemistry

The subcutaneous tumor specimens, lung, heart, liver and kidney obtained from the animal model were preserved in paraformaldehyde. Then, these tissues were embedded in paraffin and sliced (4–5 μm) for immunohistochemical staining with proliferation-related antibodies (Ki-67 and PCNA) and EMT-related antibody (E-cadherin). The paraffin-embedded lungs and other vital organs were subjected to hematoxylin and eosin (H&E) staining to evaluate the effect of Huaier on tumor metastasis and determine the drug safety. The expression level of each target protein was calculated by the percentage of positive staining cells in 10 random microscope high power fields (×200).

Statistical Analysis

All the statistical analyses between the control group and Huaier treatment group were conducted via GraphPad Prism 8.02 software and IBM SPSS 25.0 statistical software. Quantitative data of the experiment are represented as the mean ± standard deviation (S.D.). The statistically significant differences between the different groups were verified using nonparametric statistics. When $P < 0.05$, the results were defined as statistically significant. The Kaplan–Meier survival curves of the mice in lung metastatic model were assessed using Log rank test.

Results

Huaier Suppresses the Potential of Proliferation of CCLP1, REB and HuCCT1 Cells in vitro

After stimulation with different concentration gradients of Huaier, ranging from 0 mg/mL to 6 mg/mL for 24 h or 48 h, the inhibition of Huaier on the viability of CCA cells was assessed by CCK-8 assays. Experimental results in Figure 1A and B showed that Huaier suppressed the cell viability, and this effect was concentration and time dependent. In addition, inhibition of cell proliferation was further validated by colony formation experiments. As shown in Figure 1C and D, the potential of colony formation in CCLP1 and REB cells was significantly inhibited, this experimental result further verified the above conclusion.

Huaier Inhibits Migration and Invasion of CCLP1 and REB Cells in vitro

The remodeling efficiency of Huaier on cellular motility was quantified by wound healing and Tranwell assays. As shown in Figure 1E and F, pre-stimulation with Huaier could dramatically reduce the wound closure rate in CCLP1 and REB cells. Additionally, the Transwell results indicated that pre-stimulating cells with Huaier could observably inhibit the migration and invasion potential of CCA cells (Figure 1G and H).

Microarray Array Explores Differentially Expressed lncRNAs Between Control Group and Huaier Treatment Group

The results of high-throughput sequencing showed that among the 40,916 lncRNAs present in the current

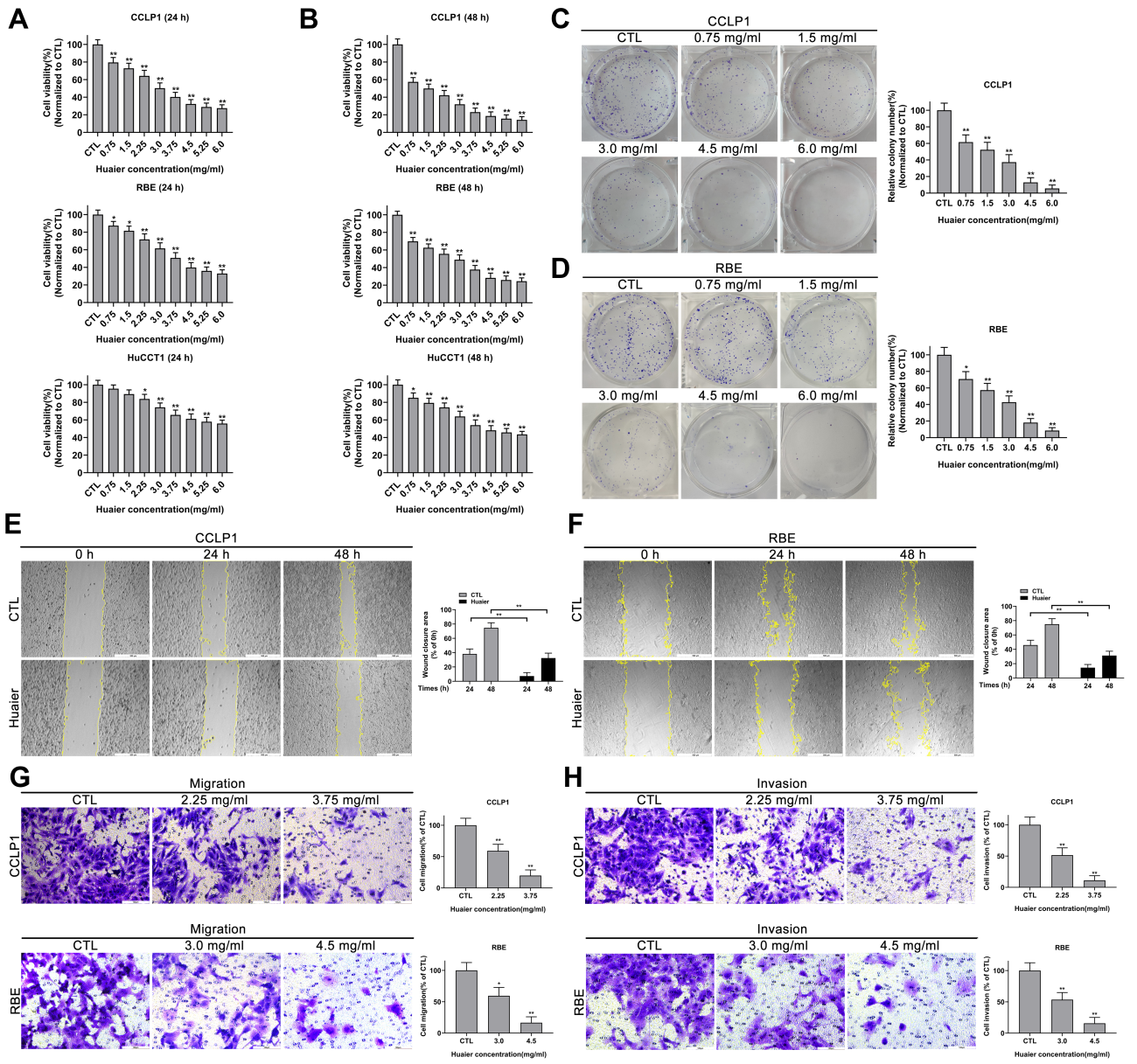

Figure 1 Huaier inhibits the proliferation, migration and invasion of cholangiocarcinoma (CCA) cells in vitro. (**A** and **B**) Cell viability curves of CCLP1, RBE and HuCCT1 cells after Huaier treatment for 24 h or 48 h were detected by CCK-8 assays. *P < 0.05, **P < 0.01 versus CTL. CTL, control. (**C** and **D**) Colony-forming abilities of CCLP1 and RBE cells after exposure to Huaier were evaluated by plate clonality assays (2 weeks of incubation). *P < 0.05, **P < 0.01 versus CTL. CTL, control. (**E** and **F**) Wound healing assays were applied to assess the effect of Huaier on mobility of CCLP1 and RBE cells. **P < 0.01. (**G** and **H**) Effect of Huaier on the migration and invasive capacities of CCLP1 and RBE cells were measured using Transwell assays. *P < 0.05, **P < 0.01 versus CTL. CTL, control. Magnification, × 40 (**E** and **F**), × 200 (**G** and **H**). Scale bar, 500 μm (**E** and **F**), 100 μm (**G** and **H**). Data are shown as mean ± SD of at least three independent experiments.

Abbreviations: SD, standard deviation; CCA, cholangiocarcinoma; CCK-8, cell counting kit-8.

microarrays, there were 227 differentially expressed lncRNAs between the control group cells and the Huaier treatment group cells (based on log fold change >2.0, $P < 0.05$). Additionally, among these differentially expressed lncRNAs, 159 were uniformly up-regulated and 68 were uniformly down-regulated. The 50 most differentially expressed lncRNAs (25 most up-regulated, 25 most down-regulated) are shown in Figure 2A by Hierarchical clustering analysis. Moreover, lncRNA TP73-AS1 with the greatest fold change was further investigated. PCR results further confirmed that TP73-AS1 was down-regulated by Huaier (2.25 mg/mL) compared with the control group. Instead, using plasmids to overexpress TP73-AS1 before Huaier treatment could make the TP73-AS1 expression level free from the interference of Huaier (Figure 2B and C).

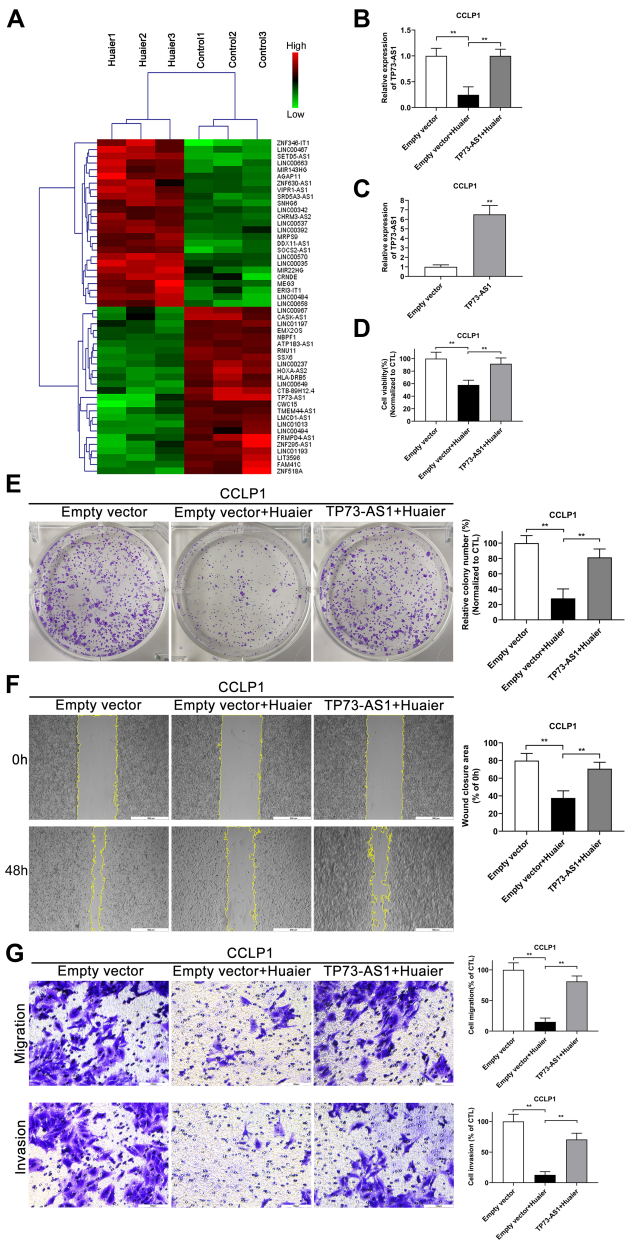

Figure 2 Huaier down-regulates the expression of lncRNA TP73-AS 1 in CCA cells. (**A**) Heat map and hierarchical clustering dendrogram of tumor-associated noncoding RNAs in CCLP1 cells pretreated with or without Huaier extract. The red color-blocks mean high expression and the green color-blocks mean low expression. (**B**) RT-qPCR analysis of TP73-AS1 expression in CCLP1 cells after Huaier treatment and TP73-AS1 overexpression. **P < 0.01. (**C**) RT-qPCR analysis of TP73-AS1 expression in CCLP1 cells after TP73-AS1 overexpression. **P < 0.01 versus empty vector control group. (**D**) Effect of TP73-AS1 overexpression on viability of Huaier-treated CCLP1 cells was evaluated by CCK-8 assays. **P < 0.01. (**E**) Effect of TP73-AS1 overexpression on proliferation abilities of Huaier-treated CCLP1 cells was detected by colony-forming tests (2 weeks of incubation). **P < 0.01. CTL, empty vector control. (**F**) Effect of TP73-AS1 overexpression on mobility of Huaier-treated CCLP1 cells was assessed by wound healing assays. **P < 0.01. (**G**) Transwell assays were performed to monitor the effect of TP73-AS1 overexpression on the migration and invasion abilities of Huaier-treated CCLP1 cells. **P < 0.01. Magnification, × 40 (**F**), × 200 (G). Scale bar, 500 μm (**F**), 100 μm (G). Mean ± SD of three independent experiments is shown.

Abbreviations: SD, standard deviation; CCA, cholangiocarcinoma; CCK-8, cell counting kit-8.

Huaier Inhibits the Malignant Biological Behaviors of CCLP1 by Down-Regulating TP73-AS1

In order to illuminate that Huaier inhibited tumor cell proliferation and metastasis by down-regulating RNA, CCK-8, colony formation, wound healing and Transwell assays were performed. As shown in Figure 2D and E, Huaier attenuated the viability of CCLP1 cells compared with the control group, instead overexpressed TP73-AS1 protected cells from the cytotoxic effects of Huaier. In wound healing and Transwell assays, the potential of migration and invasion of CCLP1 cells was suppressed by Huaier, but reversed by TP73-AS1 overexpression (Figure 2F and G). All of the above findings suggested that Huaier might play an antitumor effect through regulating lncRNA TP73-AS1 in CCA.

Knockdown of TP73-AS1 Attenuates the Malignant Biological Behaviors of CCA Cells

In a previous study, we had confirmed that TP73-AS1 was present at higher levels in CCA cells relative to human intrahepatic biliary epithelial cells (HIBEC); meanwhile, the oncogenic properties of TP73-AS1 were revealed in QBC939 and Huh-28 cells.[27] In our present research, the function of TP73-AS1 was further explored in CCLP1 cells. The results indicated that transfection with TP73-AS1 siRNA resulted in a significantly restrained CCLP1 cell viability and proliferation ability (Figure S1A–1C). Furthermore, the cellular motility and apoptosis were monitored. As shown in Figure S1D–1E, knockdown of TP73-AS1 suppressed the migration and invasion capabilities of CCLP1 cells. In addition, the apoptosis rate increased significantly after TP73-AS1 silencing in CCLP1 cells as shown in Figure S1F–1G. The results are consistent with our previous study, indicating that TP73-AS1 also plays an oncogenic function in CCLP1 cells.

Huaier Induces Oxidative Stress and Damages the Mitochondrial Membrane Potential in CCLP1 and RBE Cells

In this research, the cellular morphological changes after Huaier stimulation (2.25 mg/mL and 3.75 mg/mL for CCLP1, 3.0 mg/mL and 4.5 mg/mL for RBE) were observed. As shown in Figure 3A, Huaier caused significant changes in cell morphology, mainly including the

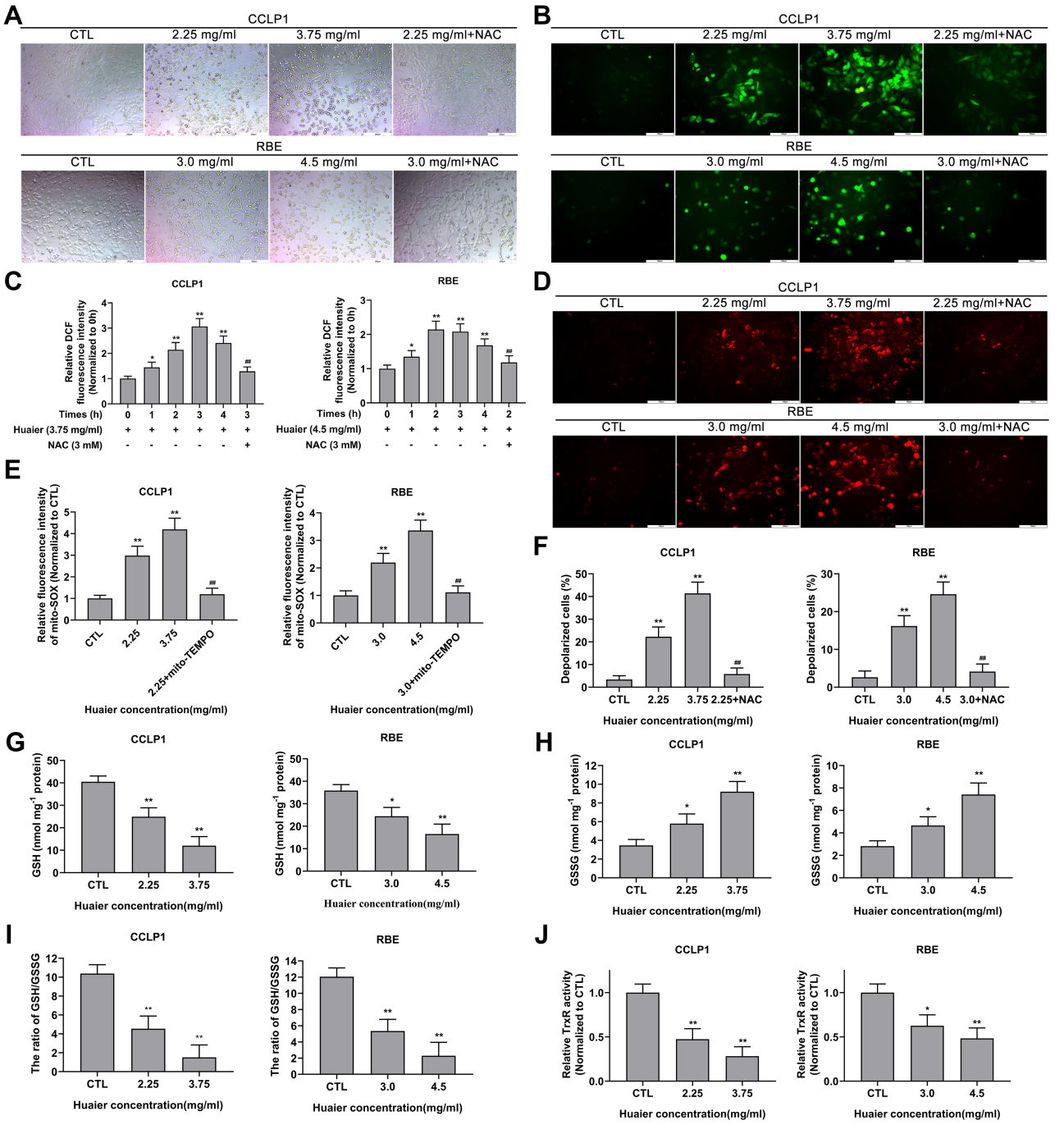

Figure 3 Huaier causes morphological change, induces oxidative stress, and unbalances the oxidation-reduction system in CCA cells. (**A**) The cellular morphological changes of CCLP1 and RBE cells caused by Huaier were analyzed by applying image analysis. (**B** and **C**) Effect of Huaier on oxidative stress levels in CCLP1 and RBE cells was initially detected by DCFH-DA fluorescent probe under inverted fluorescence microscope and microplate reader. **P* < 0.05, ***P* < 0.01 versus CTL. ##*P* < 0.01 versus Huaier (3.75 mg/mL for CCLP1) at 3 h or Huaier (4.5 mg/mL for RBE) at 2 h. CTL, control. (**D** and **E**) Effect of Huaier on oxidative stress levels in CCLP1 and RBE cells was further assessed by mito-SOX fluorescent probe under inverted fluorescence microscope and microplate reader. ***P* < 0.01 versus CTL. ##*P* < 0.01 versus Huaier (2.25 mg/mL for CCLP1 or 3.0 mg/mL for RBE) single treatment groups. CTL, control. (**F**) JC-1 probe was performed to evaluate the effect of Huaier on MMP in CCLP1 and RBE cells. ***P* < 0.01 versus CTL. ##*P* < 0.01 versus Huaier (2.25 mg/mL for CCLP1 or 3.0 mg/mL for RBE) single treatment groups. CTL, control. (**G**–**I**) The GSSG/GSH quantification kit was applied to assess the effect of Huaier on intracellular GSH, GSSG levels and the ratio of GSH to GSSG in CCLP1 and RBE cells. **P* < 0.05, ***P* < 0.01 versus CTL. CTL, control. (**J**) The thioredoxin reductase assay kit was used to detect the effect of Huaier on intracellular TrxR activity. **P* < 0.05, ***P* < 0.01 versus CTL. CTL, control. Magnification, ×100 (**A**), × 200 (**B** and **D**). Scale bar, 200 μm (**A**), 100 μm (**B** and **D**). Mean ± SD of three independent experiments is shown.

Abbreviations: SD, standard deviation; CCA, cholangiocarcinoma; DCFH-DA, 2′, 7′-dichlorofluorescein-diacetate; NAC, N-acetylcysteine; GSH, glutathione; GSSG, oxidized glutathione; TrxR, thioredoxin reductase.

decrease in cell adhesion potential and loss of normal cell morphology. In contrast, pre-stimulation with ROS scavenger (NAC 3 mM) for 2 h could rescue cells from Huaier's cytotoxicity.

Previous experiments had found that NAC protected cells from Huaier cytotoxic effects. In addition, Huaier has been shown to induce oxidative stress in human osteosarcoma and hepatocellular carcinoma. So, oxidative stress in CCLP1 and RBE cells after Huaier stimulation was initially detected using DCFH-DA probe. As shown in Figure 3B, the fluorescence intensity of DCF (bright green) was enhanced by Huaier. The fluorescence signal intensity of DCF was up-regulated as early as 1 h of Huaier stimulation (3.75 mg/mL for CCLP1 cells, 4.5 mg/mL for RBE cells), and actually peaked at 2 h (CCLP1 cells) and 3 h (RBE cells) respectively; then, gradually return to the initial level (Figure 3C). Instead, pretreatment with NAC could reverse Huaier-induced oxidative stress. In addition, the oxidative stress in CCA cells induced by Huaier was further verified by mitochondrion-specific small-molecule fluorescent probe (mito-SOX). Fluorescence detection results showed that the fluorescence signal intensity of mito-SOX (bright red) was up-regulated by Huaier (3.75 mg/mL for CCLP1 cells, 4.5 mg/mL for RBE). Additionally, it could be relieved by mito-TEMPO, a kind of mitochondrion-targeted antioxidant (Figure 3D and E).

Studies have shown that oxidative stress is closely related to the decrease of mitochondrial membrane potential. In this study, the MMP changes after Huaier stimulation were detected. As shown in Figure 3F, Huaier treatment significantly increased the number of polarized cells, and this process could be reversed by NAC. Similar results were observed in CCK-8 assay, indicating that the cytotoxicity of Huaier was indeed mediated by oxidative stress (Figure S2A).

Huaier Exhausts Intracellular GSH and Reduces TrxR Activity in CCLP1 and RBE Cells

In order to further clarify the presence of intracellular oxidative stress caused by Huaier, biochemical indicators in the REDOX system were detected. After exposure to Huaier (2.25 mg/mL and 3.75 mg/mL for CCLP1, 3.0 mg/mL and 4.5 mg/mL for RBE), the intracellular GSH concentration significantly decreased, whereas the GSSG concentration increased (Figure 3G and H). The decrease in the ratio of GSH to GSSG further confirmed the influence of Huaier on the REDOX system (Figure 3I). As shown in Figure 3J, the TrxR activity was attenuated by Huaier (2.25 mg/mL and 3.75 mg/mL for CCLP1 cells, 3.0 mg/mL and 4.5 mg/mL for RBE cells), when compared with the control group.

Huaier Induces Apoptosis in CCLP1 and RBE Cells

Due to Huaier could induce oxidative stress in CCA cells, its effect on apoptosis was initially assessed by AO/EB and Hoechst 33342 assays. The AO/EB results showed that the apoptosis rate was significantly increased after exposure to Huaier compared to the control group (Figure 4A). In contrast, pretreatment with NAC could reduce the cytotoxicity induced by Huaier (Figure 4A). In addition, similar results were obtained in the Hoechst 33342 assays; Huaier could induce changes in nuclear morphology and staining, indicating an increase in apoptosis (Figure 4B). Flow cytometry (Annexin V-FITC and PI double staining) was used for further confirming the Huaier-induced apoptosis. Experimental results suggested that Huaier could induce apoptosis in CCLP1 and RBE cells in a concentration-dependent manner (Figure 4C). However, NAC pretreatment could alleviate this procedure, suggesting that the Huaier-induced apoptosis was primarily mediated by oxidative stress.

Huaier Modulates the Expression of Proteins Involved in the Mitochondrial Apoptotic Pathway

In view of Huaier could induce oxidative stress and mitochondrial membrane potential destruction in CCA cells, the expression of key proteins associated with mitochondrial apoptotic pathway was assessed by immunoblotting assays (Figure 5A and B). The results confirmed that Huaier up-regulated Bax expression (Figure 5C and D), meanwhile down-regulated Bcl-2 expression (Figure 5E and F). As shown in Figure 5G and H, changes in the expression ratio of Bax to Bcl-2 resulted in the increase of mitochondrial membrane permeability, which led to the release of cytochrome c from the mitochondria into the cytoplasm. Since caspase-9 and caspase-3 are downstream executors of the mitochondrial apoptotic pathway, their activation status (cleaved caspase) was evaluated. After exposed to Huaier, the expression of cleaved caspase-9

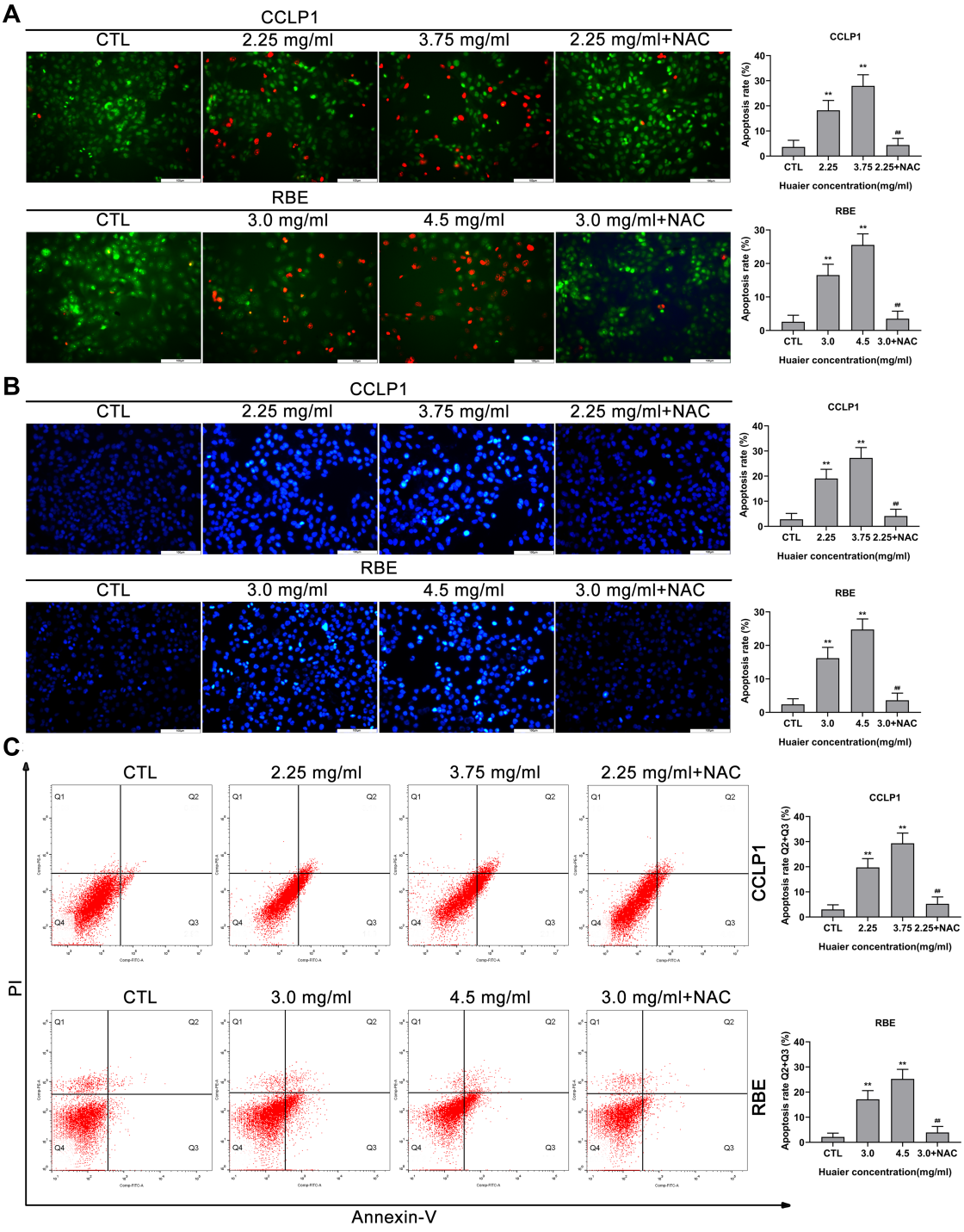

Figure 4 Huaier induces apoptosis in CCLP1 and RBE cells in vitro. (**A**) The AO/EB double-staining assays were used to test Huaier-induced apoptosis in CCLP1 and RBE cells. $^{**}P < 0.01$ versus CTL. $^{\#\#}P < 0.01$ versus Huaier (2.25 mg/mL for CCLP1 or 3.0 mg/mL for RBE) single treatment groups. CTL, control. (**B**) Huaier-induced apoptosis in CCLP1 and RBE cells was detected using Hoechst 33342 staining assays. $^{**}P < 0.01$ versus CTL. $^{\#\#}P < 0.01$ versus Huaier (2.25 mg/mL for CCLP1 or 3.0 mg/mL for RBE) single treatment groups. CTL, control. (**C**) Huaier-induced apoptosis in CCLP1 and RBE cells were analyzed using flow cytometry (Annexin V-FITC/PI double staining). Annexin V-FITC (-) and PI (-) cells were classified as alive, Annexin V-FITC (+) but PI (-) cells were classified as early apoptosis, Annexin V-FITC (+) and PI (+) cells were defined as late apoptosis. Annexin V-FITC (-) and PI (+) cells were defined as necrosis. The total rate of apoptosis was the sum of early apoptosis and late apoptosis. $^{**}P < 0.01$ versus CTL. $^{\#\#}P < 0.01$ versus Huaier (2.25 mg/mL for CCLP1 or 3.0 mg/mL for RBE) single treatment groups. CTL, control. Magnification, × 200 (**A** and **B**). Scale bar, 100 μm (**A** and **B**). Data are shown as mean ± SD of at least three independent experiments.

Abbreviations: SD, standard deviation; AO/EB, acridine orange/ethidium bromide.

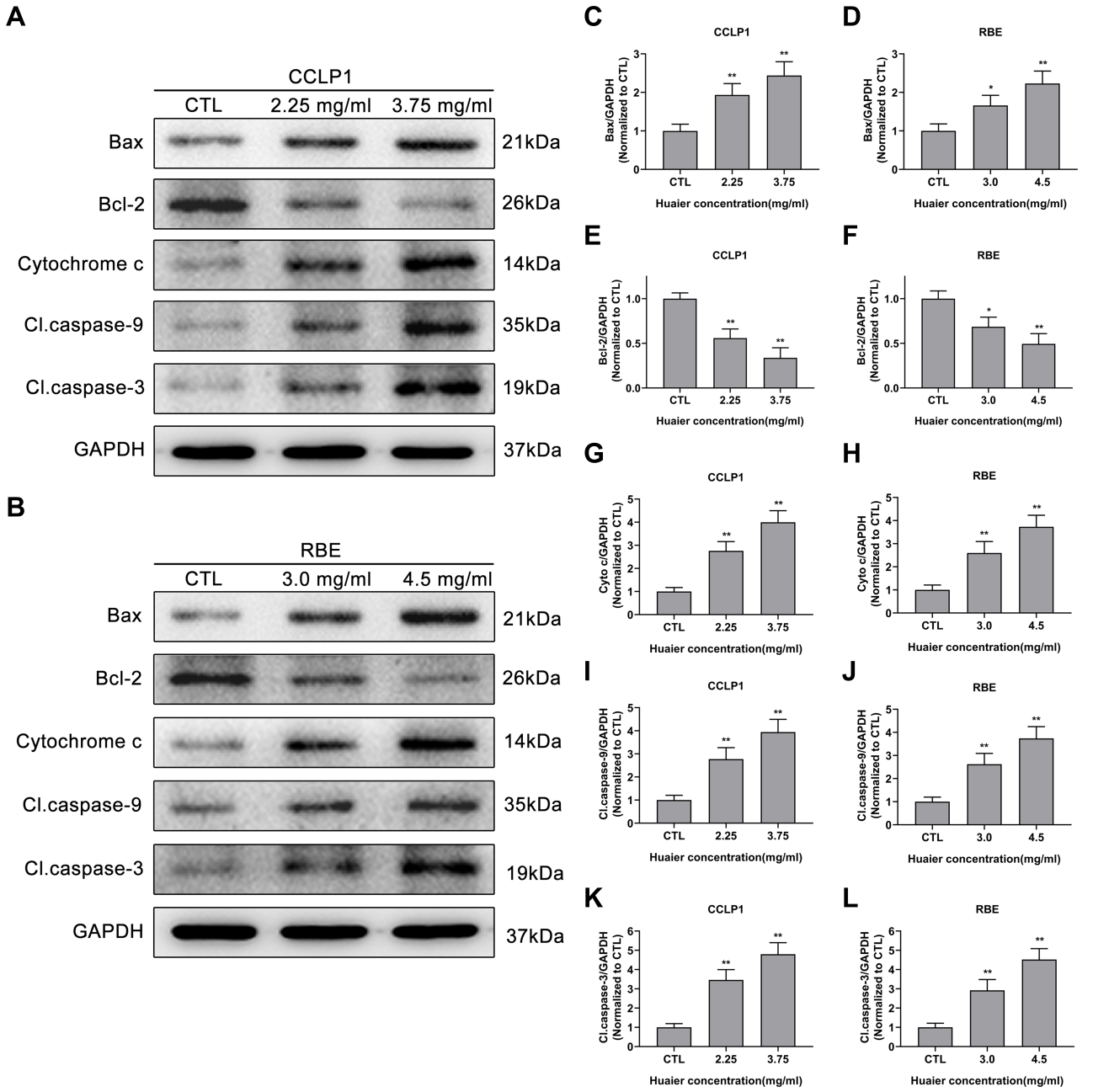

Figure 5 Effect of Huaier on the expression levels of proteins in the mitochondrial apoptotic pathway. (**A** and **B**) Huaier modulated apoptosis-related proteins in CCLP1 and RBE cells in a concentration-dependent manner. Quantitative statistics of immunoblotting analysis for Bax levels (**C** and **D**), Bcl-2 levels (**E** and **F**), cytochrome c levels (**G** and **H**), cleaved caspase-9 levels (**I** and **J**) and cleaved caspase-3 levels (**K** and **L**), $^{*}P < 0.05$, $^{**}P < 0.01$ versus CTL. CTL, control. Data are shown as mean ± SD of at least three independent experiments.

Abbreviations: SD, standard deviation; Cyto c, cytochrome c.

and cleaved caspase-3 was up-regulated, as shown in Figure 5I–L. Moreover, pretreating CCLP1 cells with z-VAD-fmk (100 μM), a pancaspase inhibitor, could eliminate the toxicity of Huaier (Figure S2B). The above results confirmed that Huaier-induced apoptosis was indeed mediated by activating the caspase cascade reaction (Figure S2C).

Huaier Inhibits the Growth of CCA in vivo

In the current research, a nude mouse subcutaneous tumor model was performed to verify the effect of Huaier on tumor growth. The specific experimental groups and intervention strategies are listed in Figure 6A and B. The results indicated that Huaier significantly decreased subcutaneous tumor growth rate compared with the control group (Figure 6C).

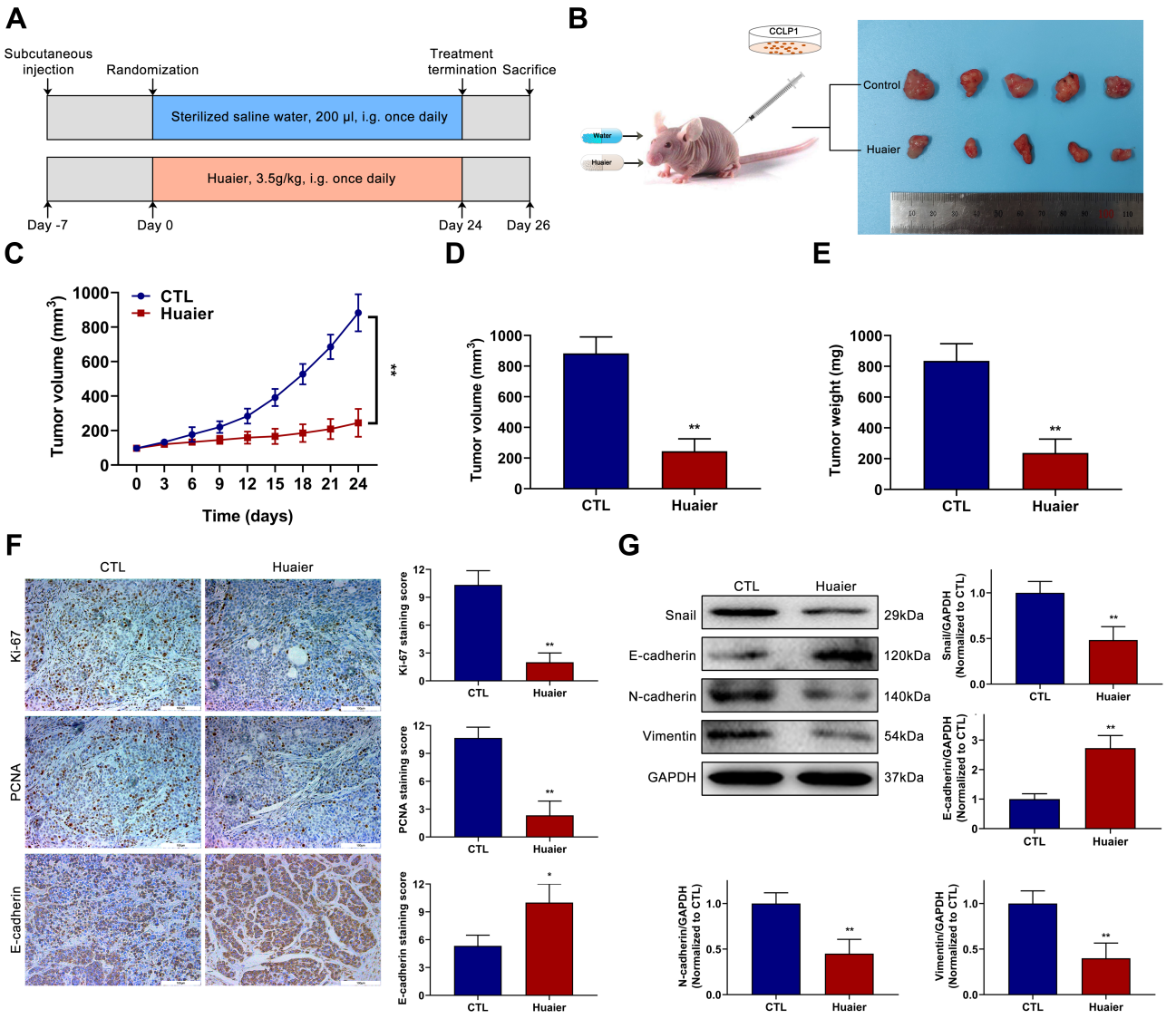

Figure 6 Huaier suppresses the growth of CCA in vivo. (**A**) The detailed grouping strategies and therapeutic schedules of subcutaneous tumor model. (**B**) Xenograft tumors were established by subcutaneous injection of CCLP1 cells (n=5). (**C**) Curves of subcutaneous tumor volume in nude mice. $^{**}P < 0.01$ versus CTL. CTL, control. (**D** and **E**) The final quantitative statistics of tumor volume and tumor weight at the end of treatment. $^{**}P < 0.01$ versus CTL. CTL, control. (**F**) Ki-67, PCNA and E-cadherin staining and quantitative statistics of the subcutaneous tumor specimens were exhibited. $^{*}P < 0.05$, $^{**}P < 0.01$ versus CTL. CTL, control. (**G**) EMT-related proteins expression levels in subcutaneous tumor specimens were evaluated and quantified by Western blotting assays. $^{**}P < 0.01$ versus CTL. CTL, control. Magnification, × 200 (**F**). Scale bar, 100 μm (**F**). Mean ± SD of three independent experiments is shown.

Abbreviations: SD, standard deviation; CCA, cholangiocarcinoma.

In addition, the tumor size and tumor weight in the medication group were also lower than these in the control group at the end of treatment (Figure 6D and E). The IHC assay showed that the expression of proliferation-related proteins (Ki-67 and PCNA) were lower, while the EMT-related protein (E-cadherin) was higher in the subcutaneous tumor specimens of Huaier therapy group compared with these of the control group (Figure 6F). In addition, the EMT-related proteins in tumor tissues were further evaluated by immunoblotting assays. Experimental results confirmed that the expression levels of Snail, N-cadherin and Vimentin were lower in the Huaier treatment group compared with these of the control group (Figure 6G). On the contrary, the expression level of N-cadherin was higher as same as that of IHC assay (Figure 6G).

Huaier Suppresses the Metastasis of CCA and Prolongs the Survival in Nude Mice with Acceptable Drug Safety

In this study, lung metastatic tumor model was applied to explore the effect of Huaier on metastasis of CCA. The

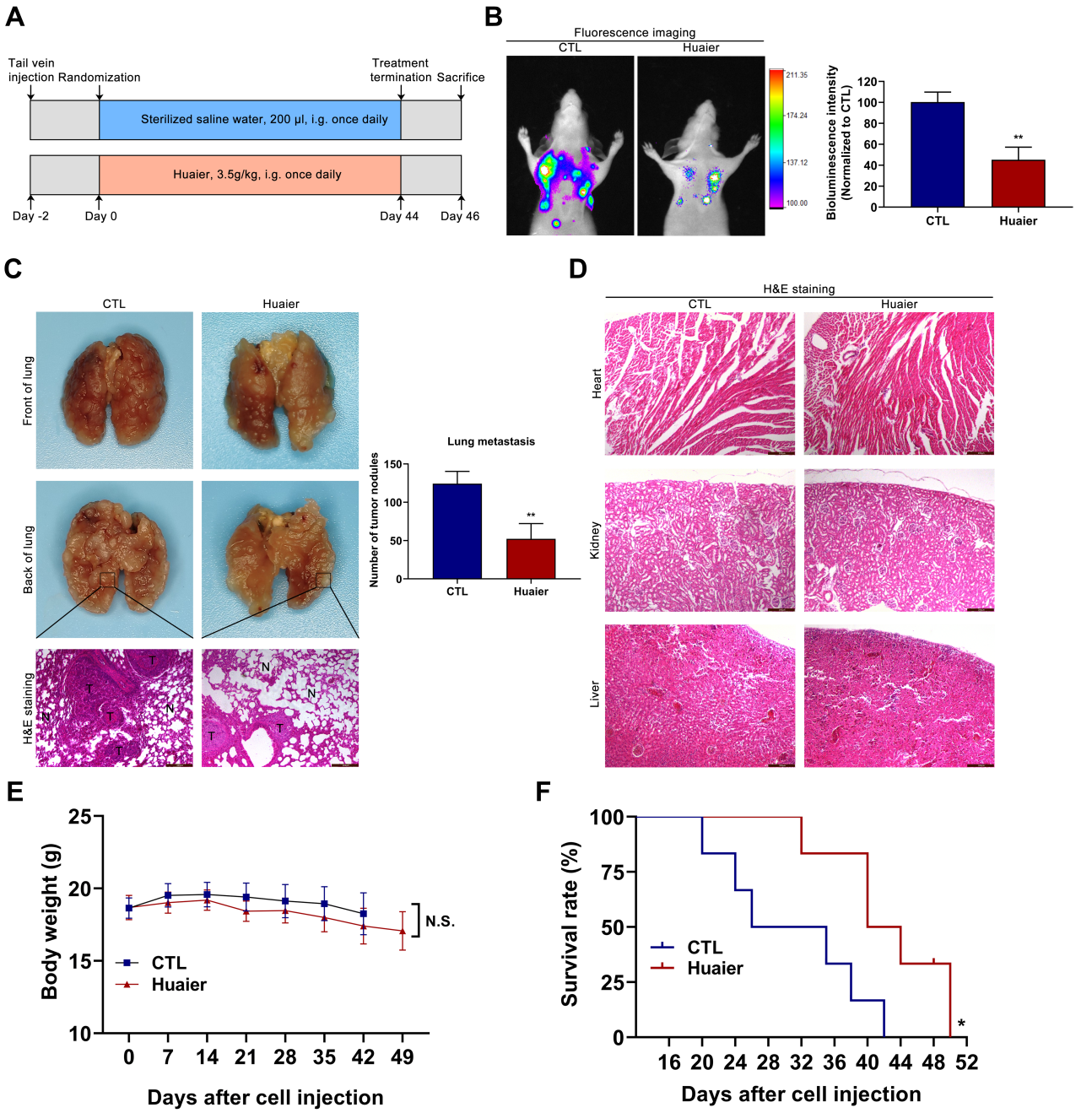

Figure 7 Huaier inhibits the metastasis of CCA in vivo. (**A**) The detailed grouping strategies and therapeutic schedules of lung metastatic model (n=5). (**B**) The therapeutic efficacy was assessed by an in vivo bioluminescence imaging system. $^{**}P < 0.01$ versus CTL. CTL, control. (**C**) Analysis of the experimental lung metastatic model was performed by injecting luciferase-labeled CCLP1 cells into the caudal vein of nude mice. $^{**}P < 0.01$ versus CTL. CTL, control. (**D**) The histology structure of heart, kidney and liver obtained from the nude mice in lung metastatic model. (**E**) Curves of average body weights in lung metastatic model (n=6). (**F**) Log rank analysis of survival rate of mice between the treatment groups (n=6). $^{*}P < 0.05$ versus CTL. CTL, control. Magnification, × 100 (**C** and **D**). Scale bar, 200 μm (**C** and **D**). Data are shown as mean ± SD of at least three independent experiments.

Abbreviations: SD, standard deviation; CCA, cholangiocarcinoma.

specific grouping strategies and treatment methods were exhibited in Figure 7A. The inhibitory effect of Huaier on tumor metastasis was detected by the in vivo bioluminescence imaging system. The data showed that the lung bioluminescence signal intensity of nude mice in the Huaier treatment group was significantly lower than that in the control group (Figure 7B). In addition, H&E staining of lung tissues further confirmed the above experimental results. The number of pulmonary metastatic nodules in the Huaier treatment group was fewer than that in the control

group (Figure 7C). The normal alveolar structure was more fully preserved in the Huaier treatment group compared with the control group (Figure 7C). The above experiments indicate that Huaier significantly inhibited tumor metastasis.

This study also provided a preliminary assessment of Huaier drug safety in vivo trials. The heart, kidney and liver obtained from the lung metastatic tumor model were examined using H&E staining assay. There was no significant difference in the intrinsic structure of these organs between the control group and the Huaier treatment group, suggesting that the drug safety of Huaier was acceptable in vivo (Figure 7D).

In order to further demonstrate the antitumor effect of Huaier in CCA, survival and quality of life in nude mice were evaluated via the lung metastatic tumor model. Body weight analysis showed that there was no significant weight change in the Huaier-treated group compared to the control group (Figure 7E). In addition, the survival time of mice in the Huaier treatment group was significantly longer than that of the control group (Figure 7F).

Discussions

Malignant tumor is one of the leading causes of human death on the world scale.[28] Although CCA accounts for only 2% of all malignancies, it ranks second among hepatic malignancies.[29] At present, in addition to surgical excision, chemotherapy is another important method to treat CCA, which could prolong survival and improve prognosis for CCA patients.[30] Despite some chemotherapeutic drugs have been confirmed to play antitumor effects in CCA, they are still toxic to normal cells.[31,32] Severe side effects of agent will lead to the interruption of chemotherapy and thus attenuate the chemotherapeutic efficacy.[33,34] Therefore, seeking new low toxicity chemotherapy agents and therapeutic targets are urgent to improve the prognosis of CCA patients.

In recent years, traditional Chinese medicine (TCM) has gained extensive attention from researchers.[35,36] More and more investigations suggested that TCM has great potential in the prevention and therapy of malignancies.[37,38] Huaier granule is the aqueous product of Huaier extract, which is approved by the National Medical Products Administration (NMPA) to be applied alone or combined with other chemotherapeutic agents in the treatment of malignant tumors.[39] In addition, recent pharmacological studies have revealed that the main active constituent of Huaier extract is polysaccharide protein (PS-T), including 6 monosaccharides and 18 amino acids. The specific content is 41.5% polysaccharides, 12.93% amino acids and 8.72% water, and the relative molecular weight is 30,000.[39] Meanwhile, other studies suggested that a neutral water-soluble polysaccharide (W-NTRP), which is isolated from the fruit bodies of Huaier and confirmed to be an arabinogalactan mainly consisting of galactose and arabinose, could inhibit the proliferation of CCA cells in a concentration-dependent manner.[40] Similar studies have been done in hepatocellular carcinoma, Huaier polysaccharide (HP), which consists of 56.2% carbohydrates, 19.2% proteins and 23.4% uronic acid, could suppress tumor metastasis.[41] Studies also indicated that some bioactive components of Huaier during extraction with water might be lost; By refining the extraction process and using different extraction solvents, researchers found that flavonoids, which make up 51.4% of the Huaier n-butanol extract, could play a role in inhibiting the proliferation and metastasis of gastric cancer cells.[42] Although there have been many studies on the bioactive components of Huaier, the basic research and clinical application on its anticancer effects are mainly based on the aqueous product of Huaier extract. With the in-depth study of Chinese medicine components and pharmacology, the antitumor and immune conditioning effects of Huaier have been gradually revealed.[38] In studies of breast cancer, hepatocellular carcinoma and renal cancer, Huaier could inhibit cell proliferation, induce cell cycle arrest and apoptosis, enhance immunocyte function and suppress metastasis.[43–45] Cumulative studies showed that Huaier could exert antitumor effects through modulating multiple classical signaling pathways and molecular targets, such as pAKT/mTOR/S6, ER/NF-κB, Wnt/β-catenin and GSK3β/β-catenin pathways.[38] Furthermore, few studies have reported that Huaier could inhibit the malignant biological behavior of tumors by regulating non-coding RNAs, including lncRNA-H19 and linc00339.[26,46] Until now, the underlying molecular mechanisms have not been completely revealed, especially in CCA. In our current study, we investigated the effects of Huaier on the malignant biological behaviors of CCA and explored lncRNAs associated with proliferation, migration, and invasion using microarray technology. In the present study, Huaier was shown to be effective in inhibiting the ability of migration and invasion of CCA cells. This is closely related to Huaier's potential to suppress the EMT process, which was revealed in the nude mice subcutaneous tumor model. In addition, CCK-8 and colony formation assays showed that Huaier could down-regulate cell viability and

cause cell damage, which might also have a close relationship with the decreased ability of tumor cell migration and invasion. However, at present, the correlation between cell viability and cell migration or invasion is not completely clear, further studies are needed to explore it in the future.

LncRNAs are a series of RNAs that are longer than 200 nucleotides and do not encode proteins.[47] Because of the important regulatory functions, lncRNAs are involved in many biological processes and pathways, and are closely related to the occurrence and development of various diseases.[47] In this research, lncRNAs associated with Huaier's antitumor effects in CCA were initially explored through microarray analysis. After 24 h of exposure to Huaier, the expression level of lncRNA TP73-AS1 was dramatically reduced. In this study, the oncogenic effect of TP73-AS1 in CCA was confirmed again, which was consistent with our previous experimental results.[27] In addition, overexpressed TP73-AS1 could alleviate the inhibitory effects of Huaier on cell proliferation, migration and invasion, suggesting that the antitumor effect of Huaier in CCA might be mediated by modulating TP73-AS1 expression. Additionally, the more detailed mechanism between TP73-AS1 and malignant biological behavior regulated by Huaier needed to be further revealed in future studies.

Recent studies have indicated that appropriate oxidative stress is crucial for tumor cells to maintain essential proliferation and differentiation.[48] At the same time, some reports have also suggested that this trait could be applied in tumor therapy, persistently higher oxidative stress level could damage tumor cells, thus promoting apoptosis through intrinsic apoptotic pathways.[49] In our present research, the oxidative stress level of CCA cells was up-regulated by Huaier treatment. In addition, the MMP was disturbed while the apoptosis rate was enhanced after exposure to Huaier. Mitochondria play an on-off role in intrinsic apoptotic pathways, starting with a decrease in mitochondrial membrane potential.[50] Next, apoptosis was achieved by remodeling the Bcl-2 family proteins, releasing cytochrome c and activating the caspase cascade reaction. To further confirm the effect of Huaier on apoptosis, the expression of proteins involved in mitochondrial apoptotic pathway, including Bcl-2, Bax, cytochrome c, cl.caspase-9 and cl.caspase-3, was analyzed using immunoblotting tests. The results showed that Huaier down-regulated the expression of anti-apoptotic Bcl-2 and up-regulated the expression of pro-apoptotic Bax. Moreover, the expression changes of Bcl-2 and Bax promoted the mitochondrial permeability transition, which released cytochrome c from mitochondria to cytoplasm and activated caspase-9 and caspase-3. The above experimental data confirmed that Huaier induced apoptosis through mitochondrial apoptotic pathway in CCA cells.

The REDOX system plays an important role in combating oxidative damage.[51] In the present study, two key biochemical indicators of REDOX balance were detected, including GSH and TrxR. Data showed that the intracellular GSH level and TrxR activity were down-regulated by Huaier, further validating the previous conclusions.

In addition, the antitumor effect of Huaier has also been demonstrated in vivo experiments. In subcutaneous tumor model and lung metastatic tumor model, Huaier effectively inhibited tumor growth and metastasis by regulating the expression of various proteins, such as proliferation-related proteins Ki-67 and PCNA, and metastasis-associated proteins Snail, E-cadherin, N-cadherin and Vimentin. Adverse reactions of traditional chemotherapy drugs remain a challenge in the chemotherapy of CCA. In our present research, the drug safety of Huaier was monitoring in vivo. The results indicated that Huaier significantly prolonged the survival of nude mice without causing severe weight loss and organ damage. These studies suggested that Huaier might be used as a novel agent for the CCA chemotherapy. Additionally, there are still some insufficiencies in the current research. In this study, we confirmed that Huaier could effectively inhibit the malignant biological properties of CCA with lower side effects in vivo. Therefore, we wondered if it is possible to reduce the dose of traditional chemotherapy drugs and combined with Huaier, thereby obtaining better efficacy with less adverse reactions. This will play an important role in improving the current chemotherapy situation of CCA, which is the goal of our future research.

Conclusions

To sum up, our current research confirmed that Huaier could inhibit cell proliferation, invasion and metastasis by modulating TP73-AS1 expression, meanwhile promote apoptosis of CCA cells through disturbing mitochondrial function, inducing oxidative stress and activating caspases in vitro. In addition, Huaier could suppress tumor growth and metastasis by regulating the expression of proliferation and EMT-related proteins. In the meantime, Huaier prolonged the survival of nude mice in lung metastatic model with acceptable drug safety. Nevertheless, further investigations are needed to explore the more detailed mechanism between Huaier and lncRNAs. Our research lays the foundation for

the development of Huaier as a novel chemotherapeutic agent to improve the prognosis of CCA.

Highlights

1. Huaier inhibited the proliferation, migration and invasion of CCA cells by down-regulating TP73-AS1.

2. Huaier induced apoptosis of CCA cells through mitochondrial apoptotic pathway.

3. Huaier suppressed the growth and metastasis of CCA by modulating the expression of proliferation and EMT-associated proteins.

Acknowledgment

The authors would like to thank the Key Laboratory of Myocardial Ischemia, Harbin Medical University, Ministry of Education for providing experimental equipment and technical support.

Author Contributions

All authors made a significant contribution to the work reported, whether that is in the conception, study design, execution, acquisition of data, analysis and interpretation, or in all these areas; All authors reviewed and approved the final manuscript, and agree to be accountable for all aspects of the work.

Funding

This work was supported by grants from the National Natural Science Foundation of China (Grant/Award Number: 81902431); Special Project of China Postdoctoral Science Foundation (Grant/Award Number: 2019T120279); China Postdoctoral Science Foundation (Grant/Award Number: 2018M641849 and 2018M640311); Heilongjiang Postdoctoral Science Foundation (Grant/Award Number: LBH-Z18107 and LBH-Z18112); Special Project of Heilongjiang Postdoctoral Science Foundation (Grant/Award Number: LBH-TZ1016); Outstanding Youth Project of Natural Science Foundation of Heilongjiang (Grant/Award Number: YQ2019H007); Postgraduate Innovative Research Project of Harbin Medical University (Grant/Award Number: YJSCX2016-21HYD); Foundation of Key Laboratory of Myocardial Ischemia, Ministry of Education (Grant/Award Number: KF201810); The Fundamental Research Funds for the Heilongjiang Provincial Universities (Grant/Award Number: 2018-KYYWF-0511 and 2018-KYYWF-0498); Chen Xiaoping Foundation for the Development of Science and Technology of Hubei Province (Grant/Award Number: CXPJJH11800004-001 and CXPJJH11800004-003); National Key Research and Development Program of China (Grant/Award Number: 2017YFC1308600).

Disclosure

The authors declare that they have no competing interests regarding the publication of this paper or this work.

References

1. Alvaro D, Barbaro B, Franchitto A, et al. Estrogens and insulin-like growth factor 1 modulate neoplastic cell growth in human cholangiocarcinoma. *Am J Pathol*. 2006;169(3):877–888. doi:10.2353/ajpath.2006.050464
2. Razumilava N, Gores GJ. Cholangiocarcinoma. *Lancet*. 2014;383(9935):2168–2179. doi:10.1016/S0140-6736(13)61903-0
3. Saha SK, Zhu AX, Fuchs CS, Brooks GA. Forty-year trends in cholangiocarcinoma incidence in the U.S.: intrahepatic disease on the rise. *Oncologist*. 2016;21(5):594–599. doi:10.1634/theoncologist.2015-0446
4. Rizvi S, Gores GJ. Pathogenesis, diagnosis, and management of cholangiocarcinoma. *Gastroenterology*. 2013;145(6):1215–1229. doi:10.1053/j.gastro.2013.10.013
5. Rizvi S, Khan SA, Hallemeier CL, Kelley RK, Gores GJ. Cholangiocarcinoma - evolving concepts and therapeutic strategies. *Nat Rev Clin Oncol*. 2018;15(2):95–111. doi:10.1038/nrclinonc.2017.157
6. Weigt J, Malfertheiner P. Cisplatin plus gemcitabine versus gemcitabine for biliary tract cancer. *Expert Rev Gastroenterol Hepatol*. 2010;4(4):395–397. doi:10.1586/egh.10.45
7. Stein A, Arnold D, Bridgewater J, et al. Adjuvant chemotherapy with gemcitabine and cisplatin compared to observation after curative intent resection of cholangiocarcinoma and muscle invasive gallbladder carcinoma (ACTICCA-1 trial) - a randomized, multidisciplinary, multinational Phase III trial. *BMC Cancer*. 2015;15:564. doi:10.1186/s12885-015-1498-0
8. Wang D, Guo H, Yang H, Wang D, Gao P, Wei W. Pterostilbene, an active constituent of blueberries, suppresses proliferation potential of human cholangiocarcinoma via enhancing the autophagic flux. *Front Pharmacol*. 2019;10:1238. doi:10.3389/fphar.2019.01238
9. Noel P, Von Hoff DD, Saluja AK, Velagapudi M, Borazanci E, Han H. Triptolide and its derivatives as cancer therapies. *Trends Pharmacol Sci*. 2019;40(5):327–341. doi:10.1016/j.tips.2019.03.002
10. Liu J, Huang Y, Liu Y, Chen Y. Irisin enhances doxorubicin-induced cell apoptosis in pancreatic cancer by inhibiting the PI3K/AKT/NF-κB pathway. *Med Sci Monit*. 2019;25:6085–6096. doi:10.12659/MSM.917625
11. Hiradeve SM, Rangari VD. A review on pharmacology and toxicology of elephantopus scaber linn. *Nat Prod Res*. 2014;28(11):819–830. doi:10.1080/14786419.2014.883394
12. Lou C, Lu H, Ma Z, Liu C, Zhang Y. Ginkgolide B enhances gemcitabine sensitivity in pancreatic cancer cell lines via inhibiting PAFR/NF-κB pathway. *Biomed Pharmacother*. 2019;109:563–572. doi:10.1016/j.biopha.2018.10.084
13. Pan J, Yang C, Jiang Z, Huang J. Trametes robiniophila Murr: a traditional Chinese medicine with potent anti-tumor effects. *Cancer Manag Res*. 2019;11:1541–1549. doi:10.2147/CMAR.S193174
14. Ji X, Pan C, Li X, et al. Trametes robiniophila may induce apoptosis and inhibit MMPs expression in the human gastric carcinoma cell line MKN-45. *Oncol Lett*. 2017;13(2):841–846. doi:10.3892/ol.2016.5517

15. Xie HX, Xu ZY, Tang JN, et al. Effect of Huaier on the proliferation and apoptosis of human gastric cancer cells through modulation of the PI3K/AKT signaling pathway. *Exp Ther Med*. 2015;10(3):1212–1218. doi:10.3892/etm.2015.2600
16. Hu Z, Yang A, Fan H, et al. Huaier aqueous extract sensitizes cells to rapamycin and cisplatin through activating mTOR signaling. *J Ethnopharmacol*. 2016;186:143–150. doi:10.1016/j.jep.2016.03.069
17. Xie J, Zhuan B, Wang H, et al. Huaier extract suppresses non-small cell lung cancer progression through activating NLRP3-dependent pyroptosis. *Anat Rec (Hoboken)*. 2019. doi:10.1002/ar.24307
18. Hu B, Yan W, Wang M, et al. Huaier polysaccharide inhibits the stem-like characteristics of ERα-36high triple negative breast cancer cells via inactivation of the ERα-36 signaling pathway. *Int J Biol Sci*. 2019;15(7):1358–1367. doi:10.7150/ijbs.27360
19. Yang A, Fan H, Zhao Y, et al. An immune-stimulating proteoglycan from the medicinal mushroom Huaier up-regulates NF-κB and MAPK signaling via Toll-like receptor 4. *J Biol Chem*. 2019;294(8):2628–2641. doi:10.1074/jbc.RA118.005477
20. Quinn JJ, Chang HY. Unique features of long non-coding RNA biogenesis and function. *Nat Rev Genet*. 2016;17(1):47–62. doi:10.1038/nrg.2015.10
21. Cui M, You L, Ren X, Zhao W, Liao Q, Zhao Y. Long non-coding RNA PVT1 and cancer. *Biochem Biophys Res Commun*. 2016;471(1):10–14. doi:10.1016/j.bbrc.2015.12.101
22. Xu Y, Yao Y, Jiang X, et al. SP1-induced upregulation of lncRNA SPRY4-IT1 exerts oncogenic properties by scaffolding EZH2/LSD1/DNMT1 and sponging miR-101-3p in cholangiocarcinoma. *J Exp Clin Cancer Res*. 2018;37(1):81. doi:10.1186/s13046-018-0747-x
23. Sanchez Calle A, Kawamura Y, Yamamoto Y, Takeshita F, Ochiya T. Emerging roles of long non-coding RNA in cancer. *Cancer Sci*. 2018;109(7):2093–2100. doi:10.1111/cas.13642
24. Tang C, Wang Y, Zhang L, et al. Identification of novel LncRNA targeting Smad2/PKCα signal pathway to negatively regulate malignant progression of glioblastoma. *J Cell Physiol*. 2020;235(4):3835–3848. doi:10.1002/jcp.29278
25. Song Y, Sun J, Xu Y, et al. Microarray analysis of long non-coding RNAs related to microRNA-148b in gastric cancer. *Neoplasma*. 2017;64(2):199–208. doi:10.4149/neo_2017_205
26. Wang J, Wang X, Chen T, Jiang L, Yang Q. Huaier extract inhibits breast cancer progression through a LncRNA-H19/MiR-675-5p pathway. *Cell Physiol Biochem*. 2017;44(2):581–593. doi:10.1159/000485093
27. Yao Y, Sun Y, Jiang Y, Qu L, Xu Y. Enhanced expression of lncRNA TP73-AS1 predicts adverse phenotypes for cholangiocarcinoma and exerts oncogenic properties in vitro and in vivo. *Biomed Pharmacother*. 2018;106:260–266. doi:10.1016/j.biopha.2018.06.045
28. Huang DW, Huang M, Lin XS, Huang Q. CD155 expression and its correlation with clinicopathologic characteristics, angiogenesis, and prognosis in human cholangiocarcinoma. *Onco Targets Ther*. 2017;10:3817–3825. doi:10.2147/OTT.S141476
29. Khan AS, Dageforde LA. Cholangiocarcinoma. *Surg Clin North Am*. 2019;99(2):315–335. doi:10.1016/j.suc.2018.12.004
30. Doherty B, Nambudiri VE, Palmer WC. Update on the Diagnosis and Treatment of Cholangiocarcinoma. *Curr Gastroenterol Rep*. 2017;19(1):2. doi:10.1007/s11894-017-0542-4
31. Howell M, Valle JW. The role of adjuvant chemotherapy and radiotherapy for cholangiocarcinoma. *Best Pract Res Clin Gastroenterol*. 2015;29(2):333–343. doi:10.1016/j.bpg.2015.03.001
32. Dasanu CA, Majumder S, Trikudanathan G. Emerging pharmacotherapeutic strategies for cholangiocarcinoma. *Expert Opin Pharmacother*. 2011;12(12):1865–1874. doi:10.1517/14656566.2011.583919
33. Cillo U, Fondevila C, Donadon M, et al. Surgery for cholangiocarcinoma. *Liver Int*. 2019;39(Suppl 1):143–155. doi:10.1111/liv.14089
34. Chun YS, Javle M. Systemic and adjuvant therapies for intrahepatic cholangiocarcinoma. *Cancer Control*. 2017;24(3):1073274817729241. doi:10.1177/1073274817729241
35. Ling CQ, Fan J, Lin HS, et al. Clinical practice guidelines for the treatment of primary liver cancer with integrative traditional Chinese and Western medicine. *J Integr Med*. 2018;16(4):236–248. doi:10.1016/j.joim.2018.05.002
36. Qi F, Zhao L, Zhou A, et al. The advantages of using traditional Chinese medicine as an adjunctive therapy in the whole course of cancer treatment instead of only terminal stage of cancer. *Biosci Trends*. 2015;9(1):16–34. doi:10.5582/bst.2015.01019
37. Yan Z, Lai Z, Lin J. Anticancer properties of traditional Chinese medicine. *Comb Chem High Throughput Screen*. 2017;20(5):423–429. doi:10.2174/1386207320666170116141818
38. Song X, Li Y, Zhang H, Yang Q. The anticancer effect of Huaier (Review). *Oncol Rep*. 2015;34(1):12–21. doi:10.3892/or.2015.3950
39. Chen Q, Shu C, Laurence AD, et al. Effect of Huaier granule on recurrence after curative resection of HCC: a multicentre, randomised clinical trial. *Gut*. 2018;67(11):2006–2016. doi:10.1136/gutjnl-2018-315983
40. Sun Y, Sun T, Wang F, et al. A polysaccharide from the fungi of Huaier exhibits anti-tumor potential and immunomodulatory effects. *Carbohydr Polym*. 2013;92(1):577–582. doi:10.1016/j.carbpol.2012.09.006
41. Zheng J, Li C, Wu X, et al. Huaier polysaccharides suppresses hepatocarcinoma MHCC97-H cell metastasis via inactivation of EMT and AEG-1 pathway. *Int J Biol Macromol*. 2014;64:106–110. doi:10.1016/j.ijbiomac.2013.11.034
42. Wang Y, Lv H, Xu Z, et al. Huaier n-butanol extract suppresses proliferation and metastasis of gastric cancer via c-Myc-Bmi1 axis. *Sci Rep*. 2019;9(1):447. doi:10.1038/s41598-018-36940-w
43. Kong X, Ding X, Yang Q. Identification of multi-target effects of Huaier aqueous extract via microarray profiling in triple-negative breast cancer cells. *Int J Oncol*. 2015;46(5):2047–2056. doi:10.3892/ijo.2015.2932
44. Shan L, Li Y, Jiang H, et al. Huaier restrains proliferative and migratory potential of hepatocellular carcinoma cells partially through decreased yes-associated protein 1. *J Cancer*. 2017;8(19):4087–4097. doi:10.7150/jca.21018
45. Wei C, Liu Z, Li L, Zhang Y, Fang Z, Fan Y. The anticancer effect of Huaier extract in renal cancer 786-O cells. *Pharmacology*. 2018;102(5–6):316–323. doi:10.1159/000492935
46. Wang W, Wang X, Li C, et al. Huaier suppresses breast cancer progression via linc00339/miR-4656/CSNK2B signaling pathway. *Front Oncol*. 2019;9:1195. doi:10.3389/fonc.2019.01195
47. Jathar S, Kumar V, Srivastava J, Tripathi V. Technological developments in lncRNA biology. *Adv Exp Med Biol*. 2017;1008:283–323.
48. Klaunig JE. Oxidative stress and cancer. *Curr Pharm Des*. 2018;24(40):4771–4778. doi:10.2174/1381612825666190215121712
49. Postovit L, Widmann C, Huang P, Gibson SB. Harnessing oxidative stress as an innovative target for cancer therapy. *Oxid Med Cell Longev*. 2018;2018:6135739. doi:10.1155/2018/6135739
50. Feng Y, Wang Y, Jiang C, et al. Nicotinamide induces mitochondrial-mediated apoptosis through oxidative stress in human cervical cancer HeLa cells. *Life Sci*. 2017;181:62–69. doi:10.1016/j.lfs.2017.06.003
51. Gesslbauer B, Bochkov V. Biochemical targets of drugs mitigating oxidative stress via redox-independent mechanisms. *Biochem Soc Trans*. 2017;45(6):1225–1252. doi:10.1042/BST20160473